









# Ultra-High precision Compton polarimetry at 2 GeV

Mark Dalton for

J.C. Cornejo, C. Gal, D. Gaskell, M. Gericke, I. Halilovic,  
H. Liu, J. Mammei, R. Michaels, C. Palatchi, J. Pan, K.D.  
Paschke, S. Premathilake, A. Zec, B. Quinn, and J. Zhang



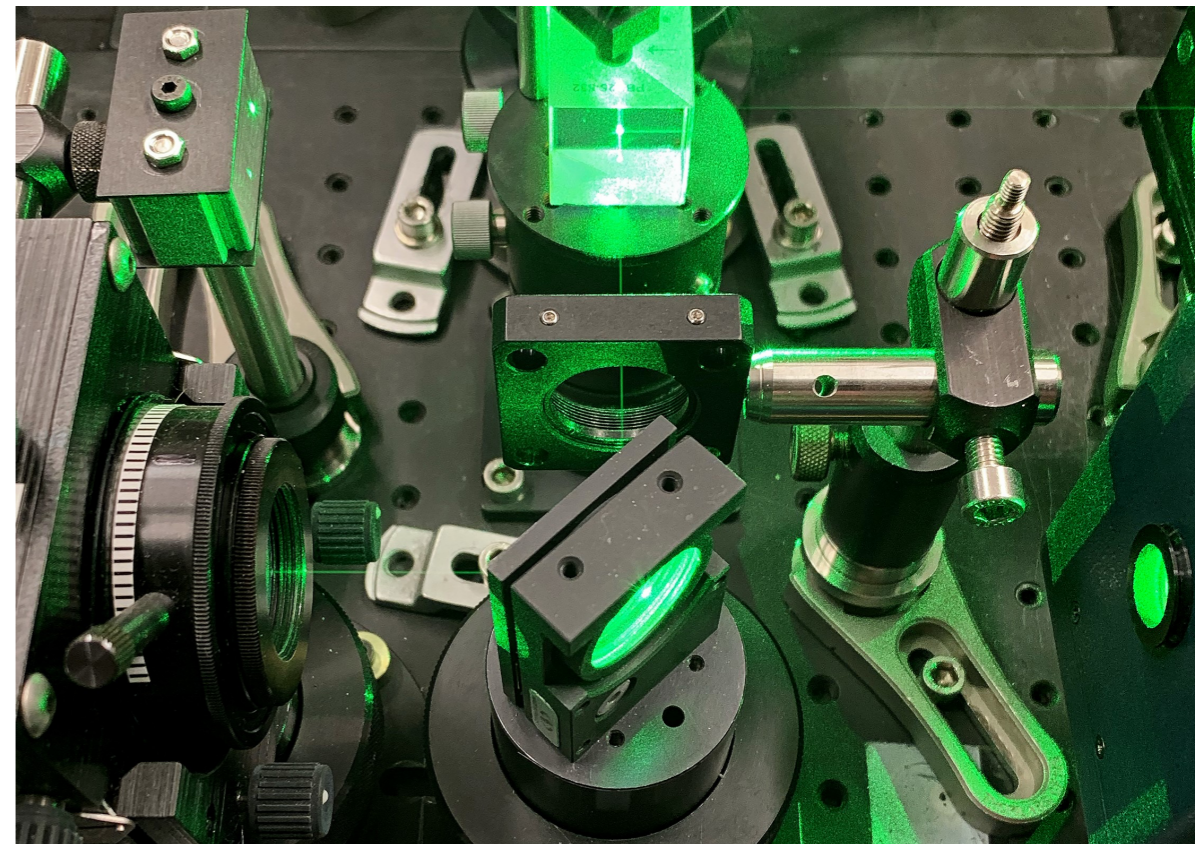
## Ultrahigh-precision Compton polarimetry at 2 GeV

A. Zec <sup>1</sup>, S. Premathilake,<sup>1</sup> J. C. Cornejo,<sup>2</sup> M. M. Dalton <sup>3,\*</sup>, C. Gal <sup>1,3,4,5</sup>, D. Gaskell <sup>3</sup>, M. Gericke <sup>6</sup>, I. Halilovic,<sup>6</sup>  
H. Liu,<sup>7</sup> J. Mammei,<sup>6</sup> R. Michaels,<sup>3</sup> C. Palatchi,<sup>1,5</sup> J. Pan,<sup>6</sup> K. D. Paschke <sup>1</sup>, B. Quinn <sup>2</sup>, and J. Zhang <sup>4,5,8</sup>

We report a high precision measurement of electron beam polarization using Compton polarimetry. The measurement was made in experimental Hall A at Jefferson Lab during the CREX experiment in 2020. A total uncertainty of  $dP/P = 0.36\%$  was achieved detecting the back-scattered photons from the Compton scattering process. This is the highest accuracy in a measurement of electron beam polarization using Compton scattering ever reported, surpassing the groundbreaking measurement from the SLD Compton polarimeter. Such uncertainty reaches the level required for the future flagship measurements to be made by the MOLLER and SoLID experiments.

[doi:10.1103/PhysRevC.109.024323](https://doi.org/10.1103/PhysRevC.109.024323)

<https://www.jlab.org/news/releases/laser-focused-look-spinning-electrons-shatters-world-record-precision>



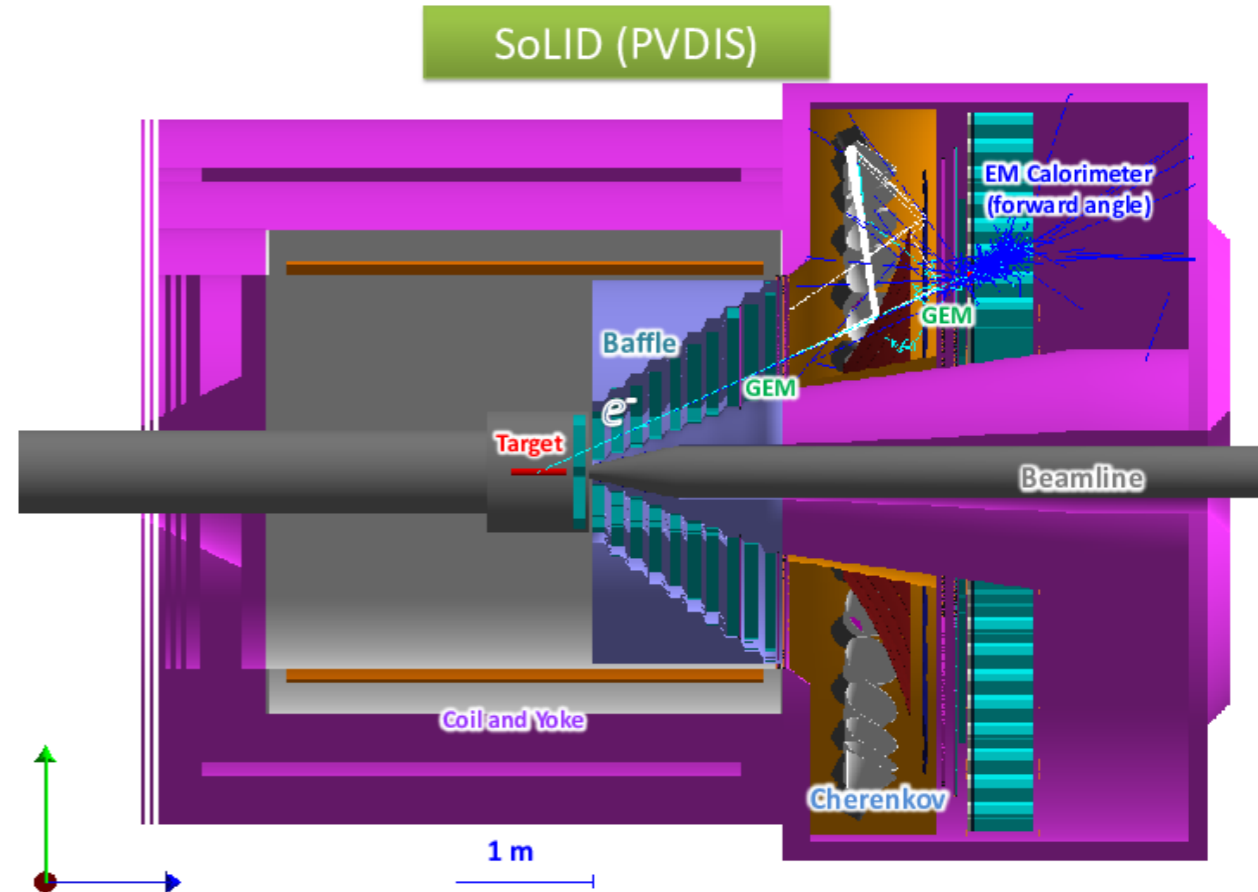
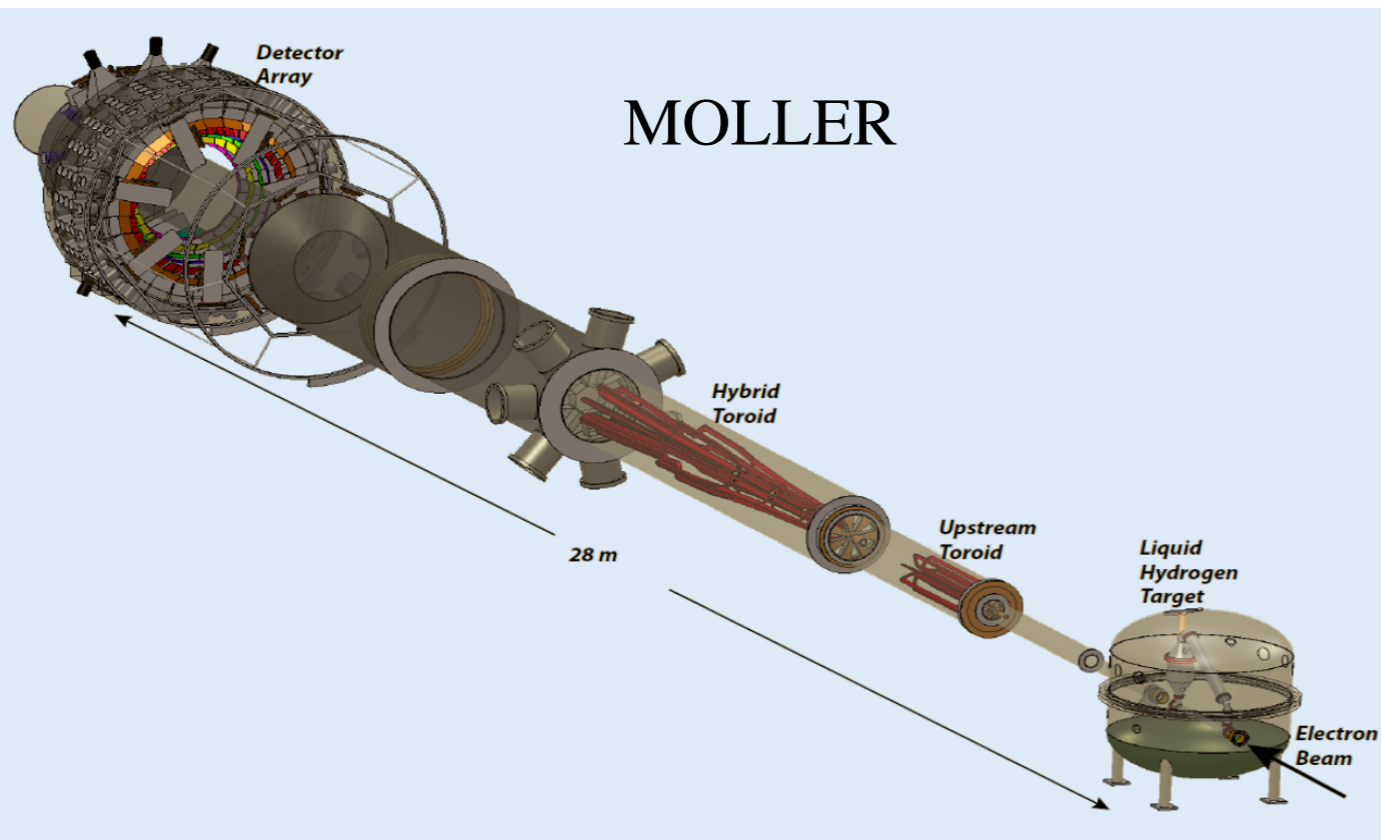
# Why Compton Polarimetry?

Polarization changes with time, constant monitoring is necessary.

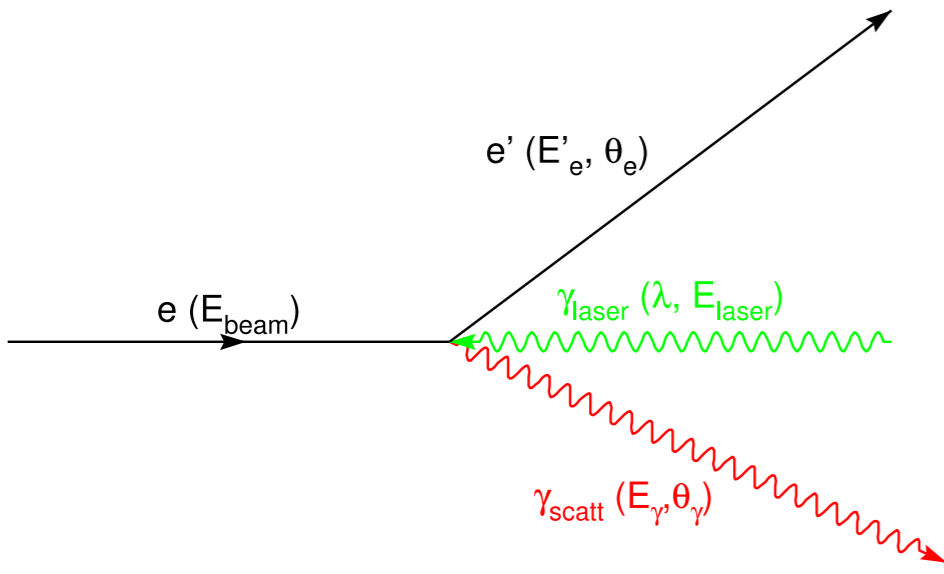
Asymmetry measurements cancel many sources of systematic uncertainty, but the polarization is a direct and often dominant source of uncertainty.

Any ultra-high precision measurement should be checked by at least one other technique and/or device of comparable precision.

Future experiments will need exquisite precision (better than 0.4 % on polarization).

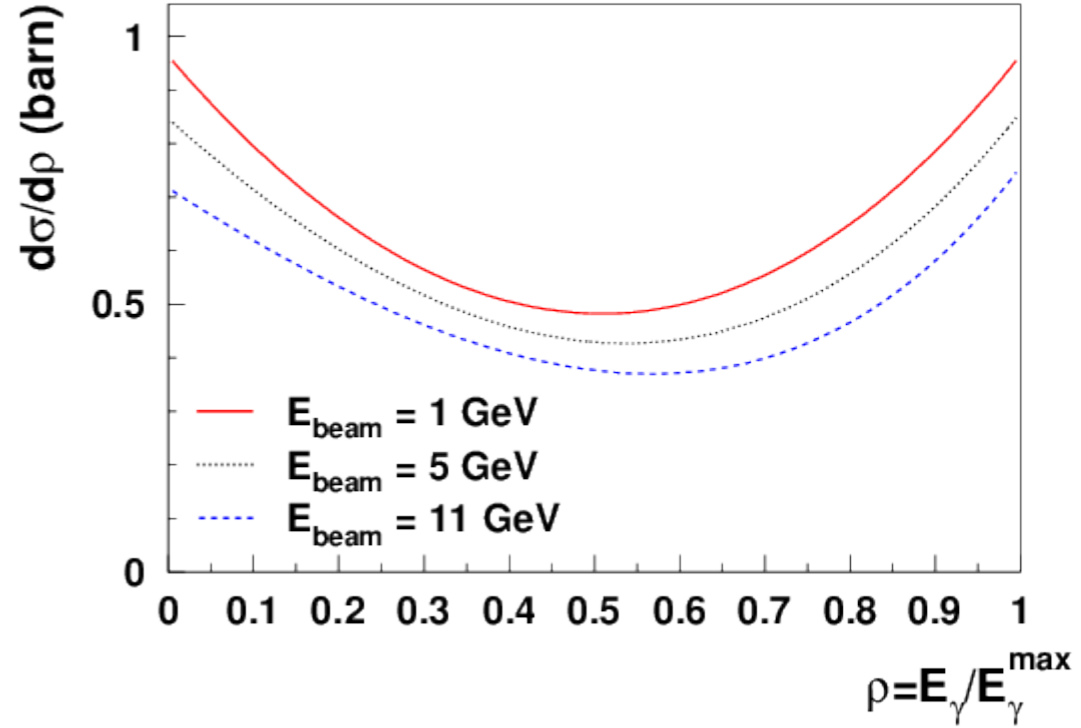


# Compton Scattering

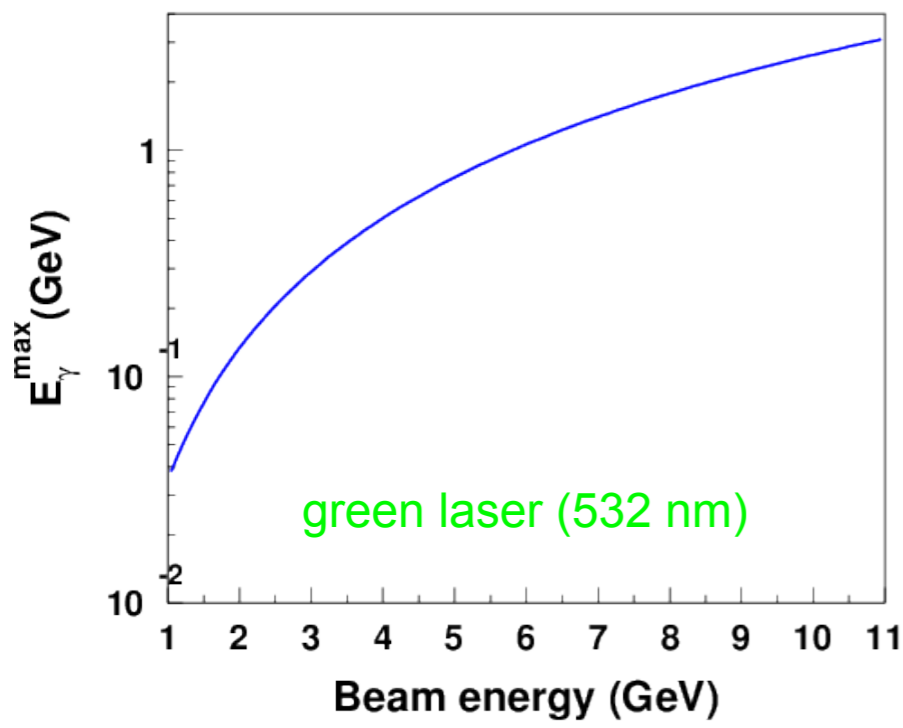


Laser beam colliding with electron beam nearly head-on

$$\frac{d\sigma}{d\rho} = 2\pi r_o^2 a \left[ \frac{\rho^2(1-a)^2}{1-\rho(1-a)} + 1 + \left( \frac{1-\rho(1+a)}{1-\rho(1-a)} \right)^2 \right]$$

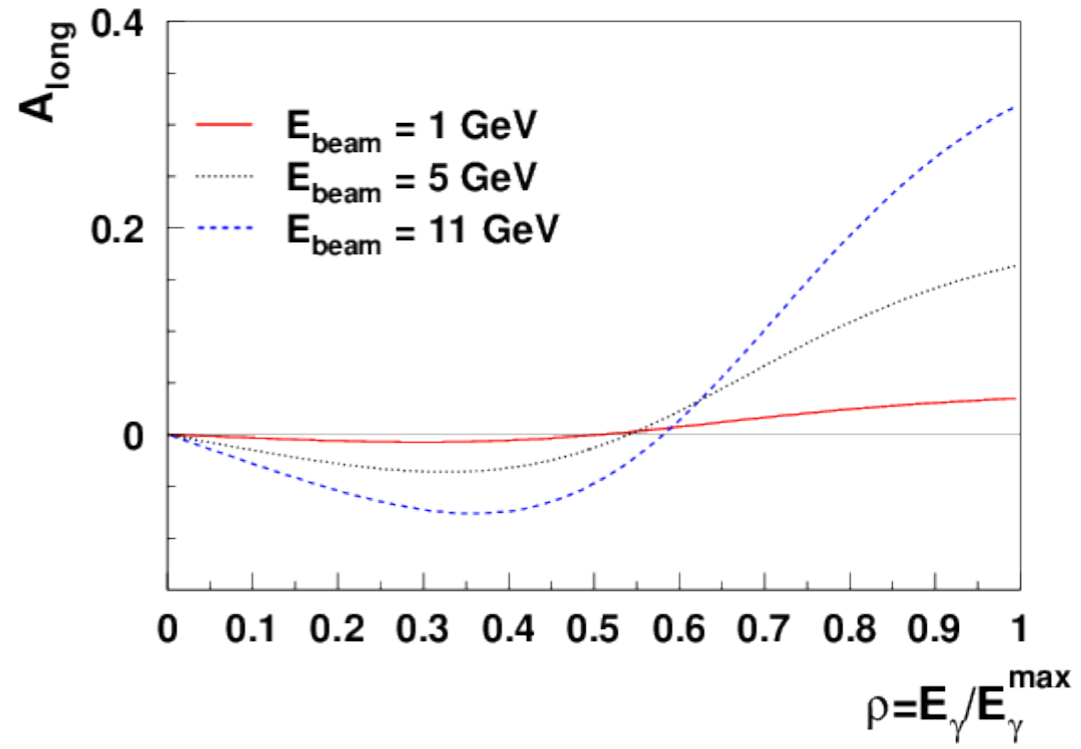


Max energy transfer at  $\theta_{\text{cm}} = 180^\circ$



$E_\gamma^{\text{max}} = 34.5 \text{ MeV}$  at  $E_{\text{beam}} = 1 \text{ GeV}$   
 $E_\gamma^{\text{max}} = 3.1 \text{ GeV}$  at  $E_{\text{beam}} = 11 \text{ GeV}$

$$A_{\text{long}} = \frac{2\pi r_o^2 a}{(d\sigma/d\rho)} (1 - \rho(1+a)) \left[ 1 - \frac{1}{(1 - \rho(1-a))^2} \right]$$



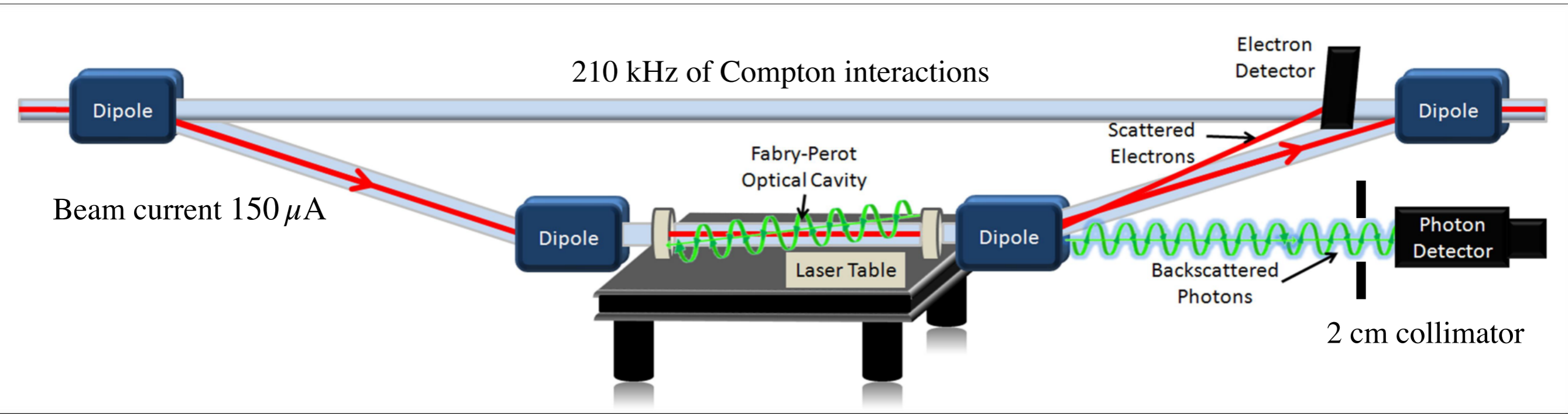
$E_\gamma^{\text{max}} = 158 \text{ MeV}$  at  $E_{\text{beam}} = 2.18 \text{ GeV}$   
 $A_{\text{max}} = 7.5 \%$   
 $\langle A_p \rangle = 3.6 \%$  full spectrum weighted by calorimeter response

# Compton Cartoon

uncertainty dominated by  
knowledge of the system  
dispersion and detector geometry

4-dipole chicane: Deflect electron beam vertically

segmented strip detector



2.2 kW of stored laser power

Ce-doped  $Gd_2SiO_5$  (GSO)  
operated in integrating mode

uncertainty dominated by  
detailed detector response

well-known QED interaction (no fundamental limit)

“nondestructive” and simultaneous

difficult to make rapid measurements

analyzing power is strongly dependent on the beam energy, and energy transfer

# Compton Polarimetry History

Polarimeter	Beam energy	Laser wavelength and technology	Detection and method	Sys. uncertainty (dP/P)
CERN LEP	46 GeV	532 nm (pulsed)	$\gamma$ /integrating	5%
HERA LPOL	27.5 GeV	532 nm (pulsed)	$\gamma$ /integrating	1.6%
HERA TPOL	27.5 GeV	514 nm (CW)	$\gamma$ /counting	2.9%
MIT-Bates	0.3–1 GeV	532 nm	$\gamma$ /counting	6%
NIKHEF	<1 GeV	514 nm	$\gamma$ /counting	4.5% @ 440 MeV
Mainz A4	0.85, 1.5 GeV	514 nm intra-cavity Ar-ion	$(\gamma, e)$ /counting	N/A
JLab Hall A	1–6 GeV	1064 nm, FP cavity	$\gamma$ /counting	3% (2002)
			$e$ /counting	1% (2006)
			$\gamma$ /integrating	1% (2009)
	1.1 GeV	532 nm, FP cavity	$\gamma$ /integrating	1.1% (2010)
JLab Hall C	1.1 GeV	532 nm, FP cavity	$e$ /counting	0.6%
			$\gamma$ /integrating	3%
SLD at SLAC	45.6 GeV	532 nm (pulsed)	$e$ /multiphoton	0.5%

Selected polarimeters emphasizing absolute beam polarization measurements.

Table from [doi: S0218301318300047](https://doi.org/10.1016/j.nima.2018.04.047) (as of 2018)

# Precision Era

Clear “high-nails” could lead to improved precision

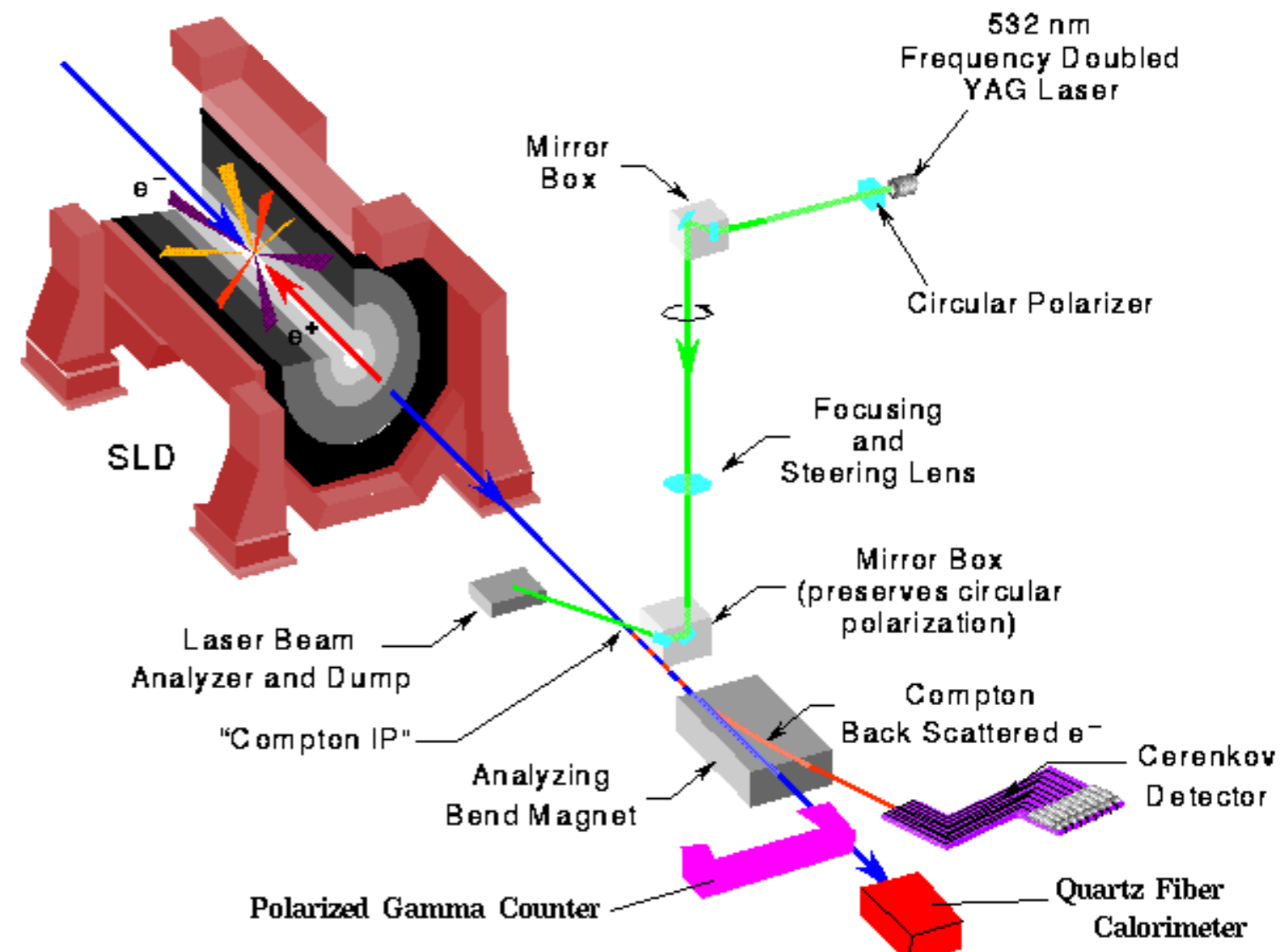
	SLD	Hall A (photon)	Hall C (electron)
<b>Properties</b>			
Beam energy	45.6 GeV	3 GeV	1.16 GeV
Endpoint $A_{\text{long}}$	74.7%	5.21%	4.06%
Laser system	532 nm, pulsed	1064 nm, FP cavity	532 nm, FP cavity
Detector	Cherenkov	GSO	Diamond strip
Scheme	Multiphoton	Integrating	Differential
<b>Uncertainties</b>			
	$dP/P$ (%)		
Laser polarization	0.10	0.80	0.18
Detector response (linearity, gain)	0.20	0.48	0.1
Analyzing power determination	0.40	0.13	0.27
DAQ and electronics related	0.20	N/A	0.48
Total	0.50	0.94	0.59

Table from [doi: S0218301318300047](https://doi.org/10.1103/PhysRevAccelBeams.21.040401) (as of 2018)

# SLD

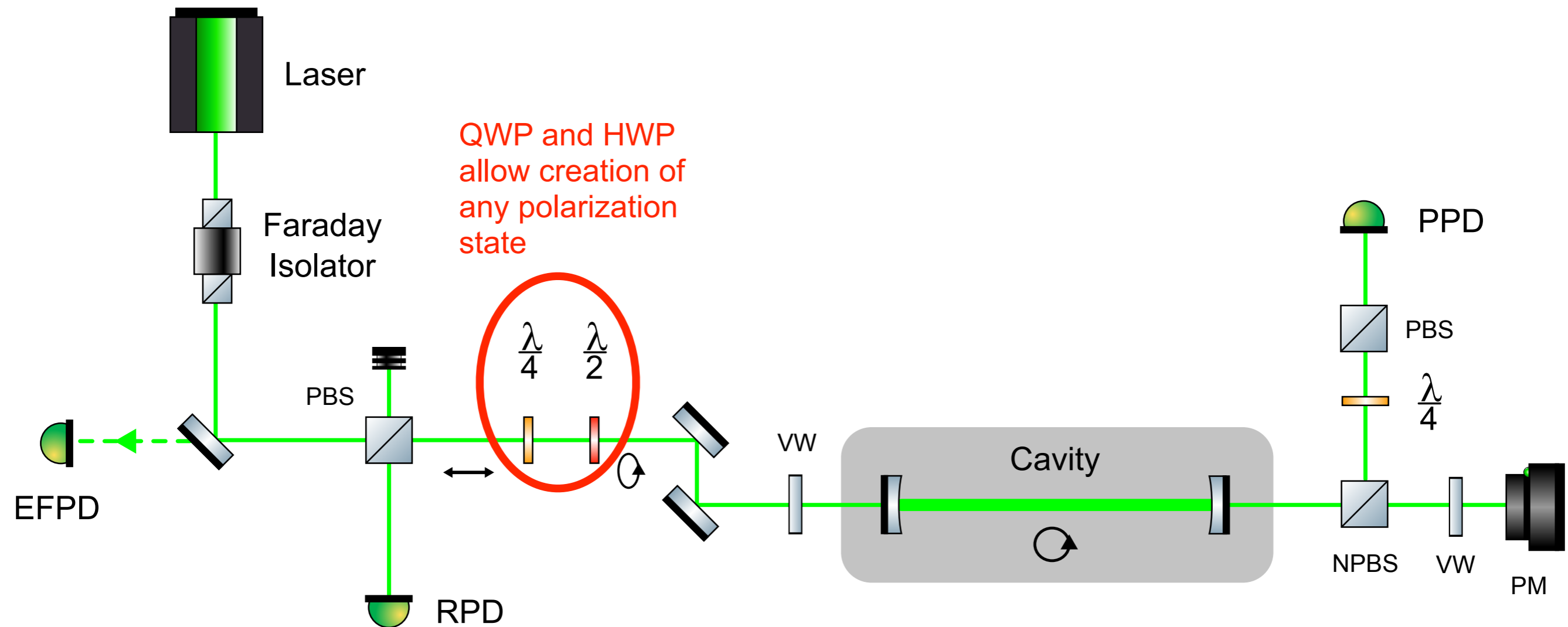
- SLD polarimeter at the SLAC Linear Collider (SLC)
- first sub-1% Compton polarization measurement (final  $dP/P = 0.5\%$ )
- statistical precision of better than 1% in a three minute run
- single-pass (pulsed) laser system - monitor laser polarization before and after interaction
- laser polarization determined to 0.1%

- segmented Cherenkov detector with each channel about 1 cm wide.
- large endpoint analyzing power ( $\approx 75\%$ )
- “multi-photon” operation: segmentation of the electron detector provides the Compton spectrum energy information, each channel provides a signal proportional to the number of scattered electrons in each bunch.





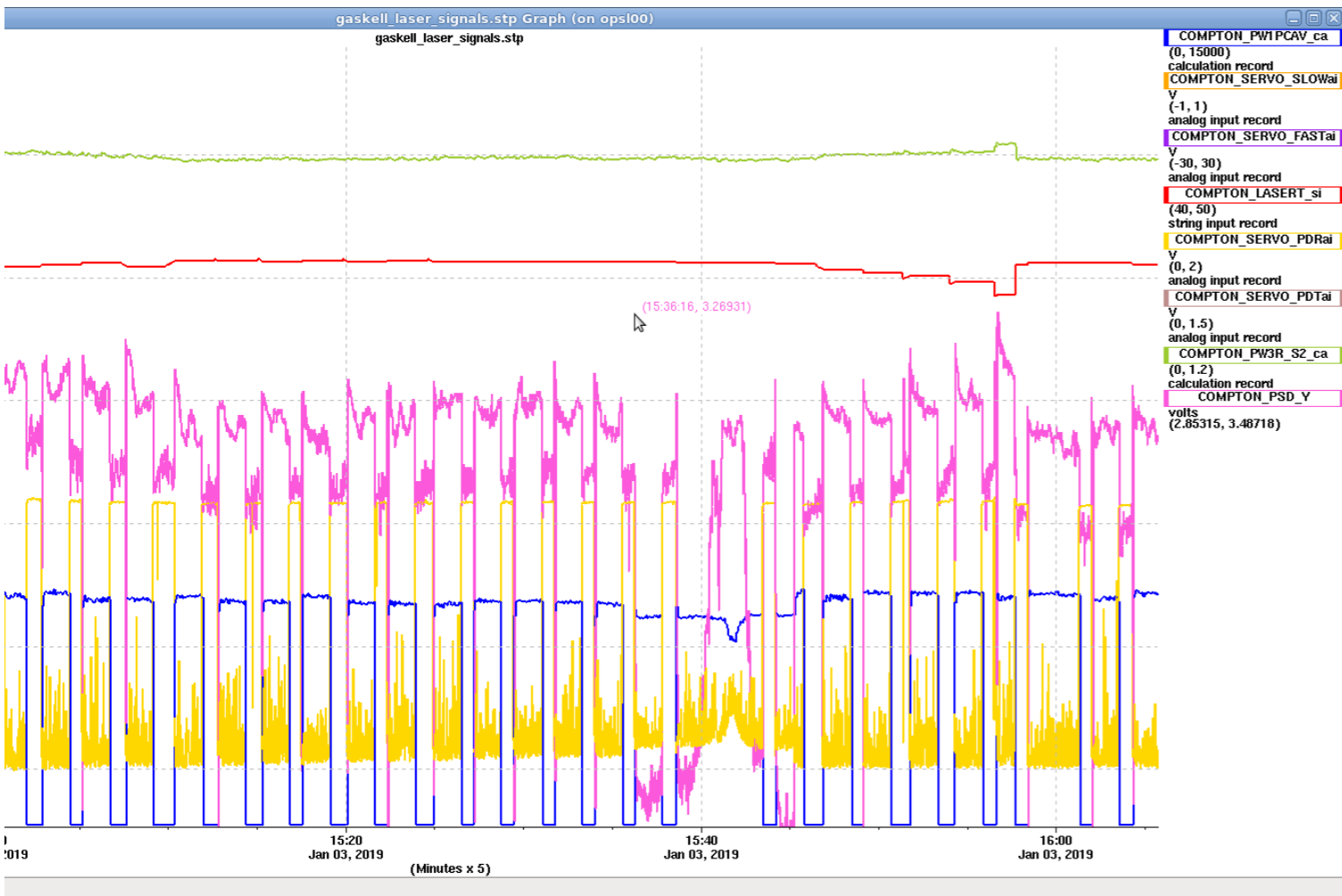
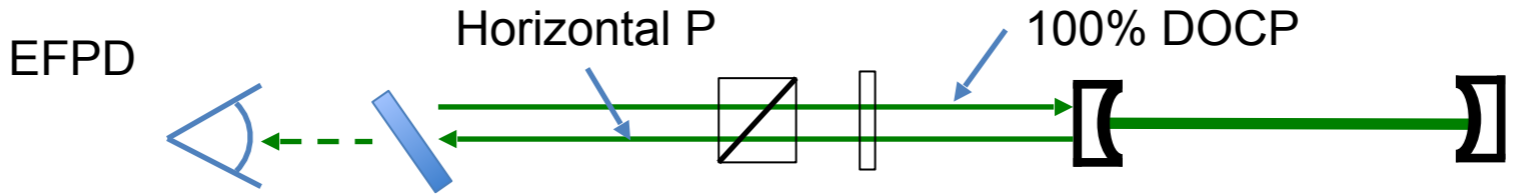
# Laser System



Optical reversibility theorem: on reflection from a mirror, the reflected laser beam can be described using the inverse of the matrix of the forward propagating beam.

# Cavity Birefringence

New observation of cavity birefringence in Hall A Fabry-Pérot Cavity



Back reflected light

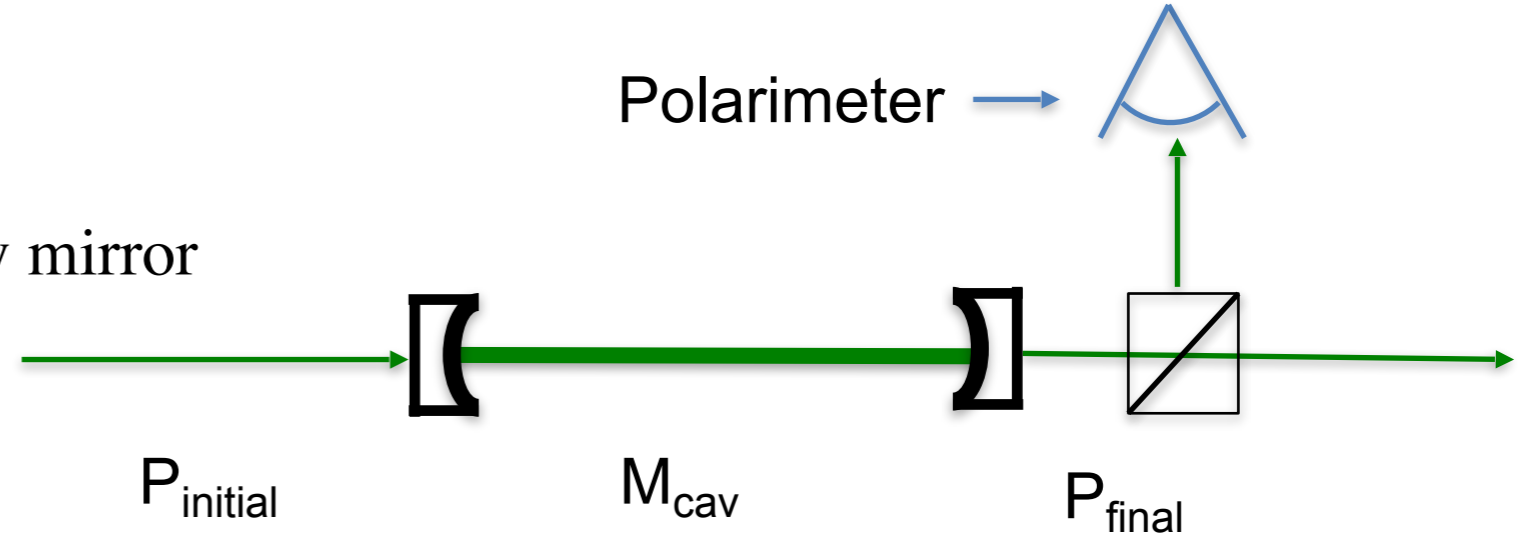
Laser power

Amount of light reflected back from cavity increases when it is locked!

# Measuring Cavity Birefringence

Cavity birefringence can be measured by:

1. Prepare known input polarization state
2. Measure polarization after second cavity mirror



Mathematically, system can be described using Jones matrix formalism

$$P_{\text{final}} = M_{\text{cav}} P_{\text{initial}}$$

$M_{\text{cav}}$  encodes total effect of birefringence due to cavity system

Parameterized:  $M_{\text{cav}} = R(\eta)PH(\delta)R(\theta)$

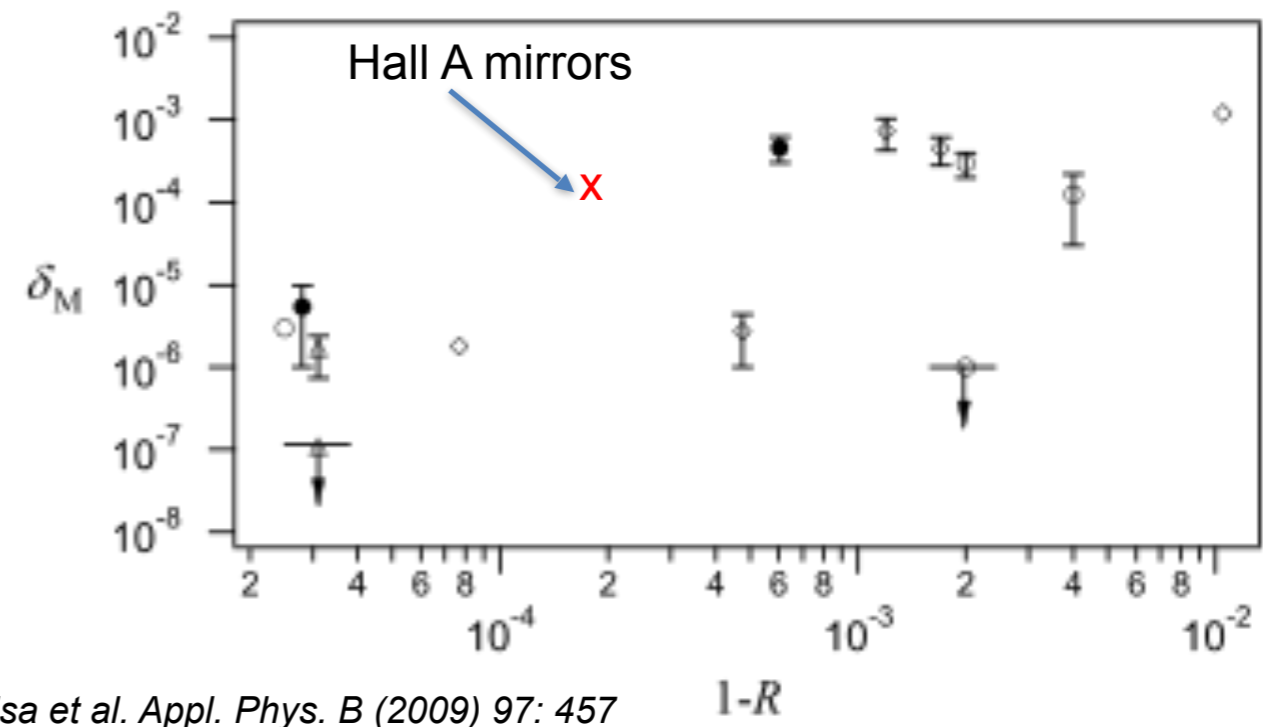


$$\delta = 1.11 \pm 0.1 \text{ degrees}$$

$$\delta_{\text{Total}} = \frac{\text{Finesse}}{2\pi} \delta_M$$

Hall A cavity: Finesse  $\sim 12000$

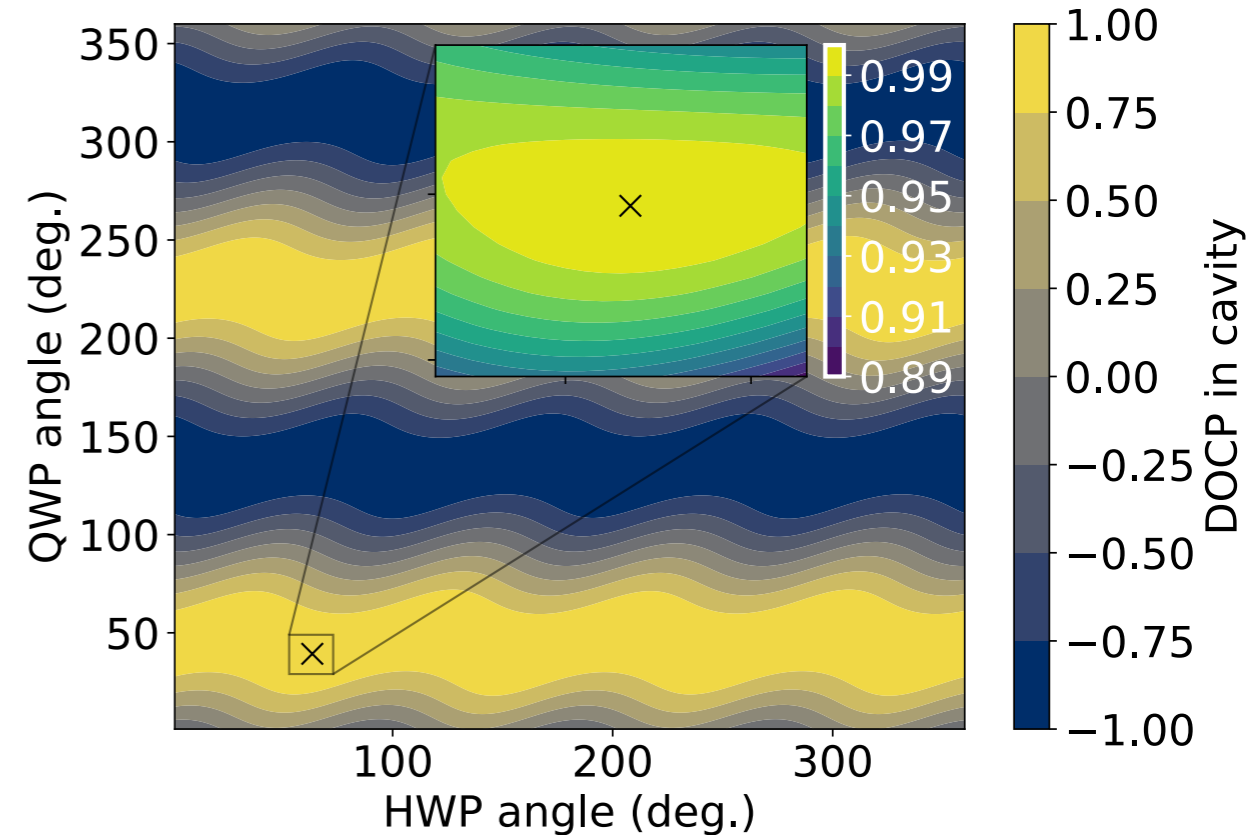
$$\delta_M = 14.5 \times 10^{-5} \text{ degrees}$$



F. Bielsa et al. Appl. Phys. B (2009) 97: 457

# Laser Operation and Systematic Uncertainty

Use knowledge of entrance function and cavity birefringence to run at  $\sim 100\%$  DOCP.

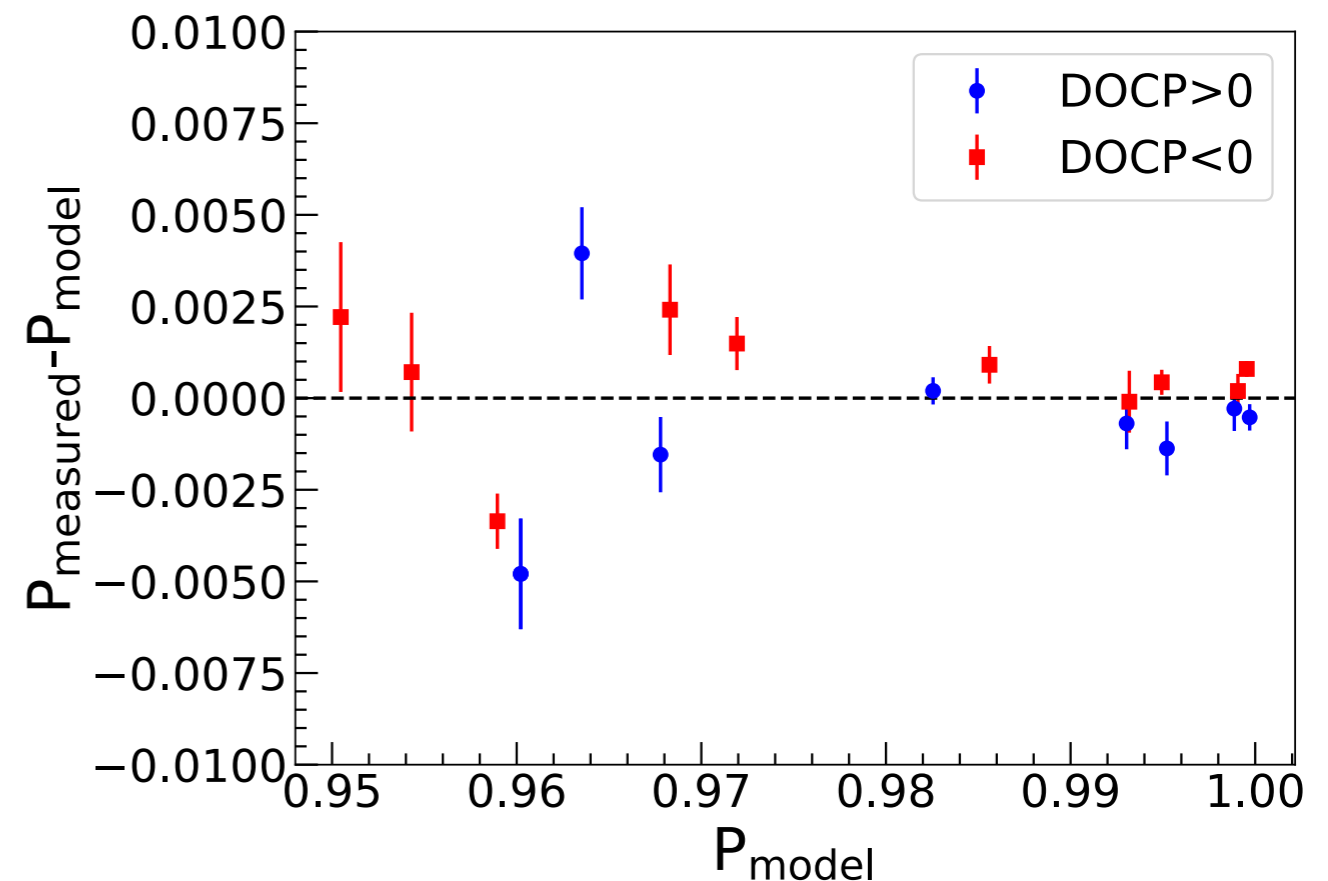


0.05% time dependence of transmitted laser polarization

0.03% uncertainties in the laser model

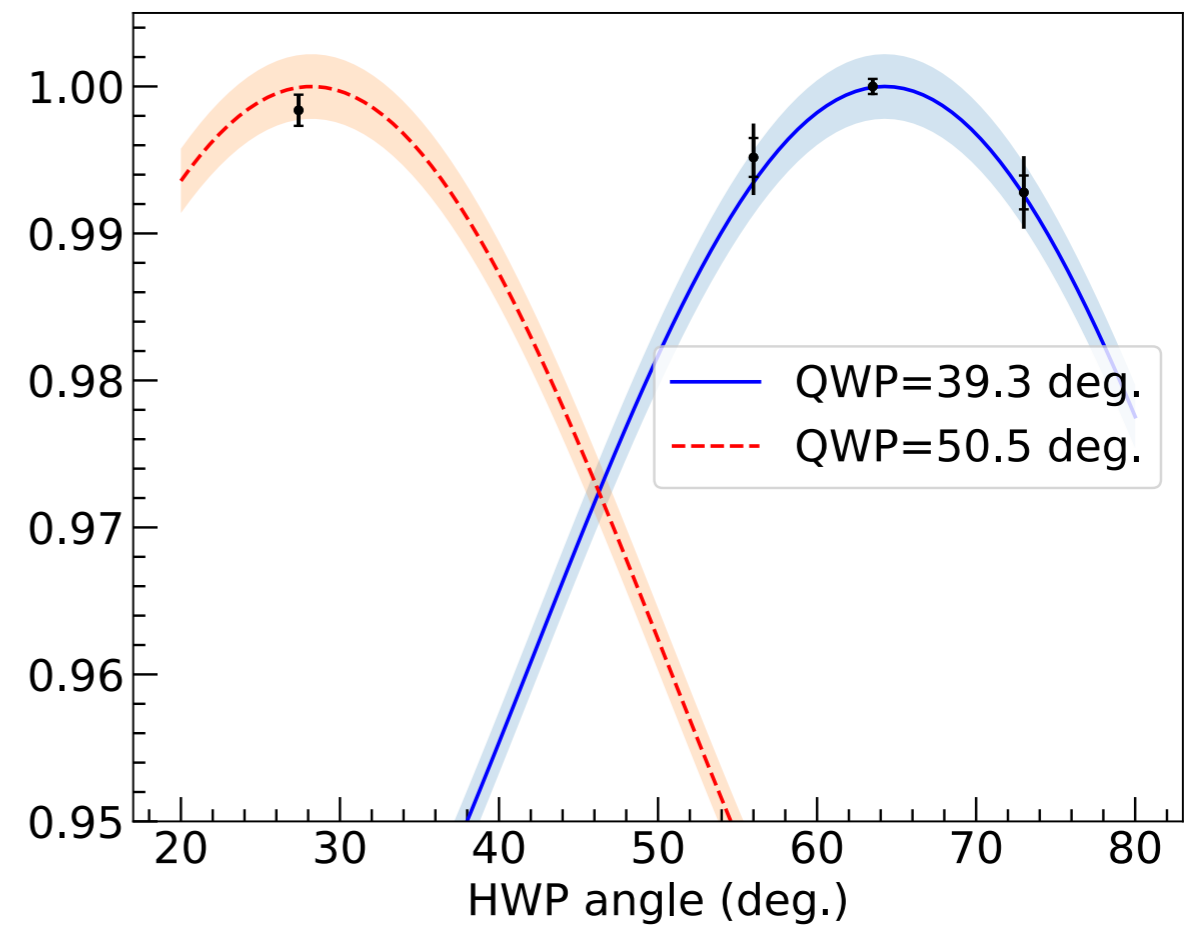
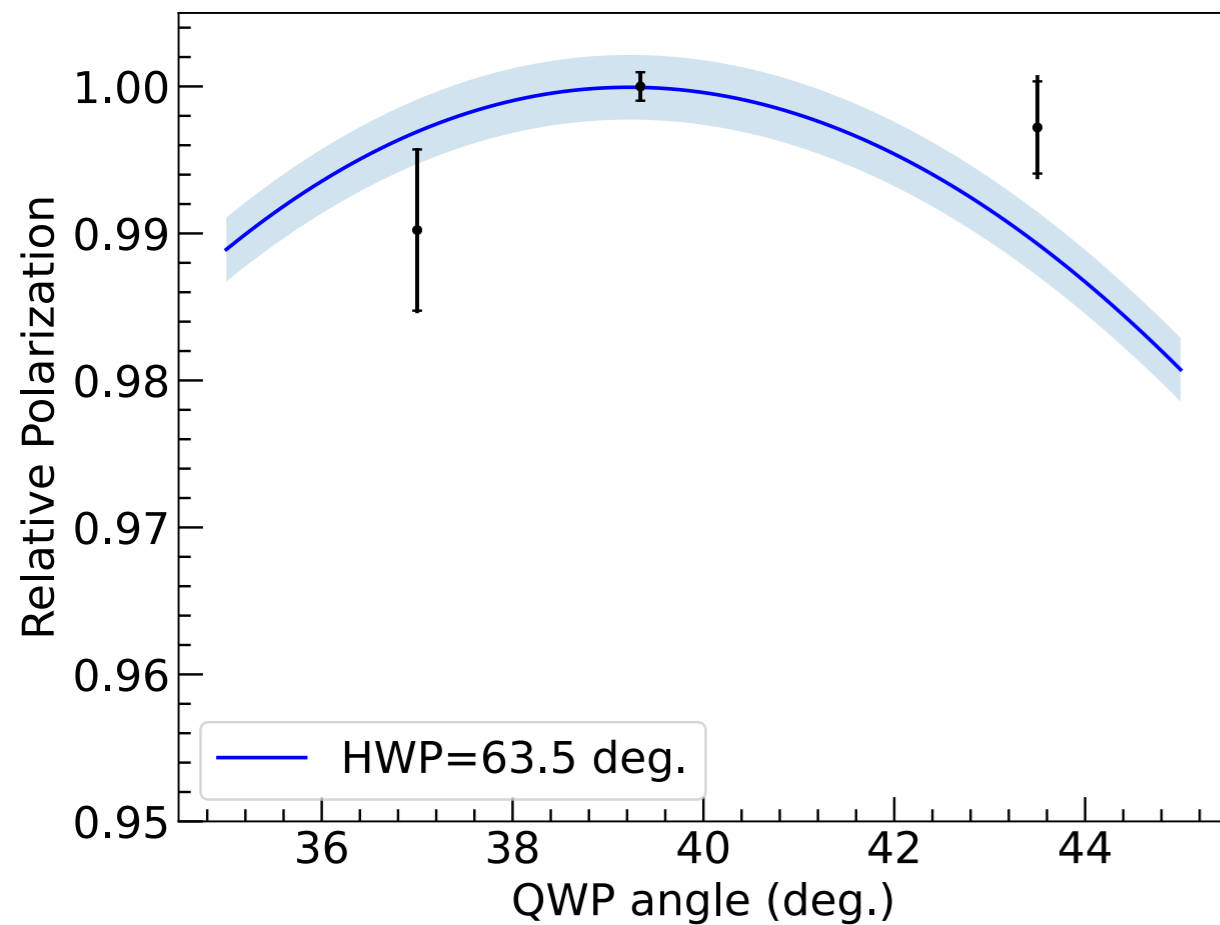
0.1% possible birefringent effects from second cavity mirror (constrained by direct measurement)

0.22% residuals of the laser model



# Testing the Laser Model

Measure Compton asymmetry with laser set to different polarization values.



# Photon Detector

$$A_{\text{meas}} = \frac{\Sigma^+ - \Sigma_-}{\Sigma^+ + \Sigma_-}$$

$$A_{\text{meas}} = A_p P_e P_\gamma$$

Measured in quartets, + - - + and - + + -  
at 120 Hz.

the analyzing power is an energy-weighted average calculated over the full energy spectrum of scattered photons

$$\langle A_p \rangle_{\text{meas}} = \frac{\int_0^{k_\gamma^{\text{max}}} A_p(k_\gamma) k_\gamma \epsilon(k_\gamma) R(k_\gamma) \sigma_0(k_\gamma) dk_\gamma}{\int_0^{k_\gamma^{\text{max}}} k_\gamma \epsilon(k_\gamma) R(k_\gamma) \sigma_0(k_\gamma) dk_\gamma} = 3.6 \%$$

$\epsilon(k_\gamma)$  acceptance

$R(k_\gamma)$  average response of the calorimeter

energy weighted has larger analyzing power and decreased sensitivity to the low energy part of the spectrum.

“threshold-less integration” technique was employed to minimize sensitivity to the absolute energy calibration of the detector

The “energy integrated” signal is sensitive primarily to knowledge of the detector linearity, which can be reliably determined via careful LED measurements.

# Asymmetry Calculation

Laser cycled on and off every 2 minutes to measure background.

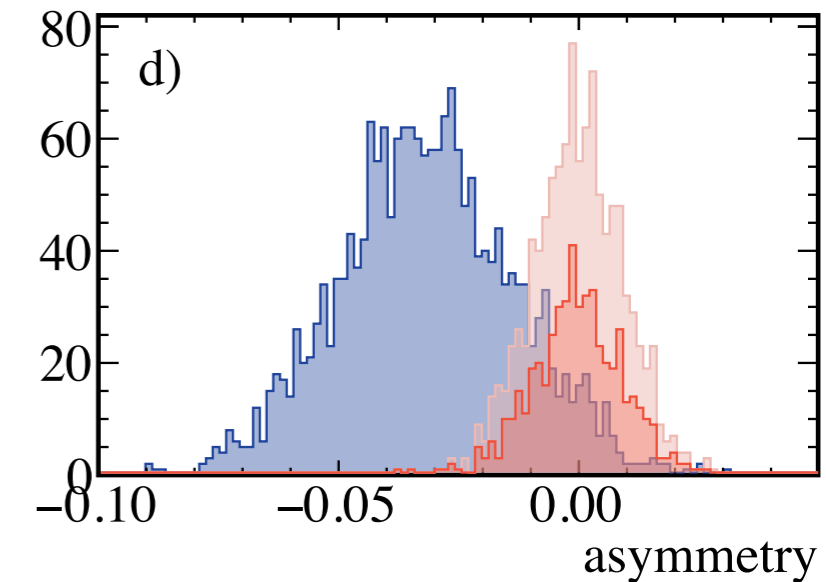
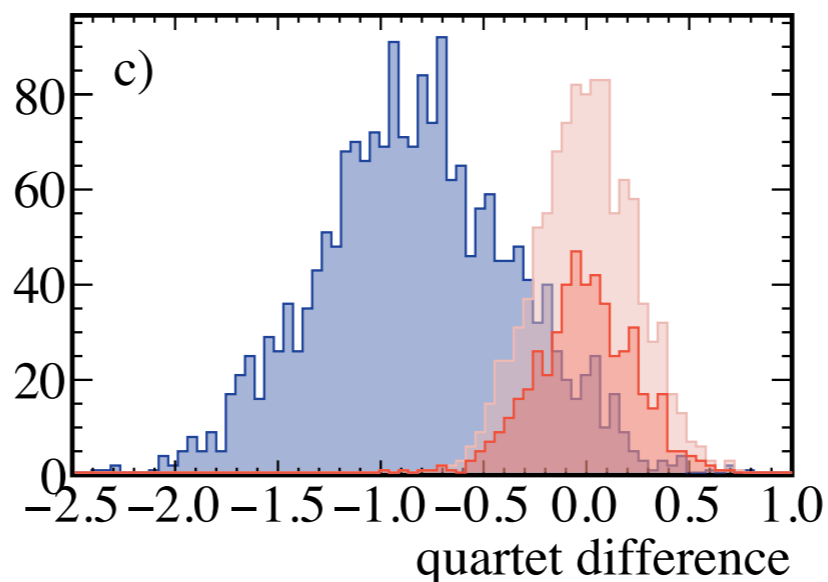
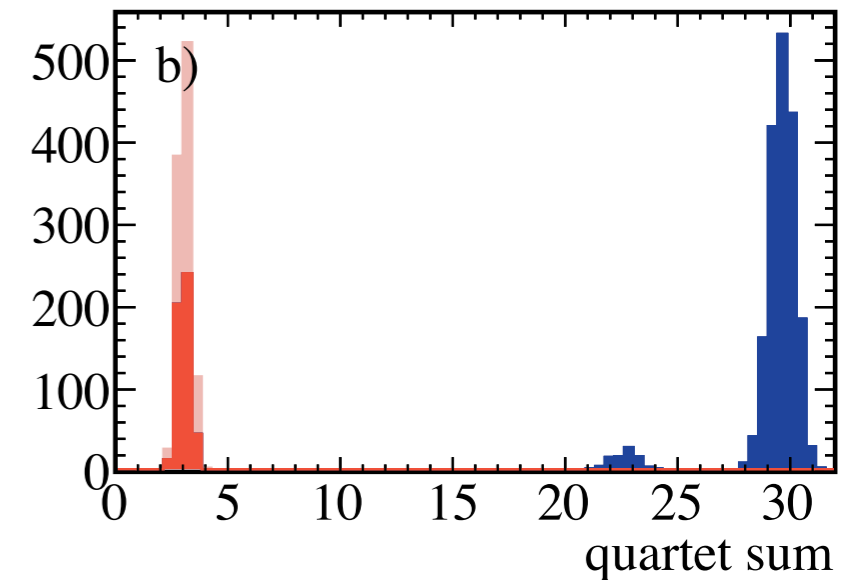
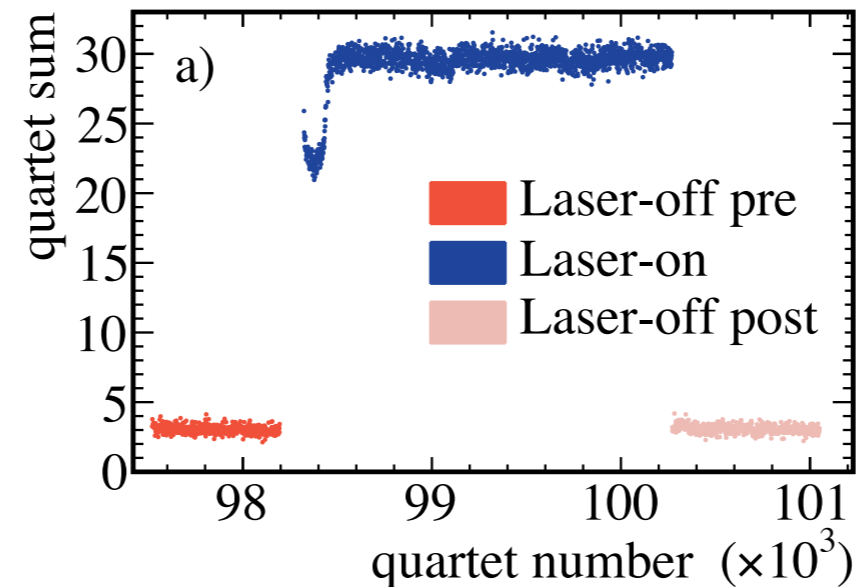
Beam trips give pedestal measurement

$$A_{\text{ON}} = \frac{\Delta_{\text{ON}}}{Y_{\text{ON}} - \langle Y_{\text{OFF}} \rangle}$$

$$A_{\text{OFF}} = \frac{\Delta_{\text{OFF}}}{\langle Y_{\text{ON}} \rangle - \langle Y_{\text{OFF}} \rangle}$$

$$A_{\text{exp}} = \langle A_{\text{ON}} \rangle - \langle A_{\text{OFF}} \rangle$$

single laser cycle

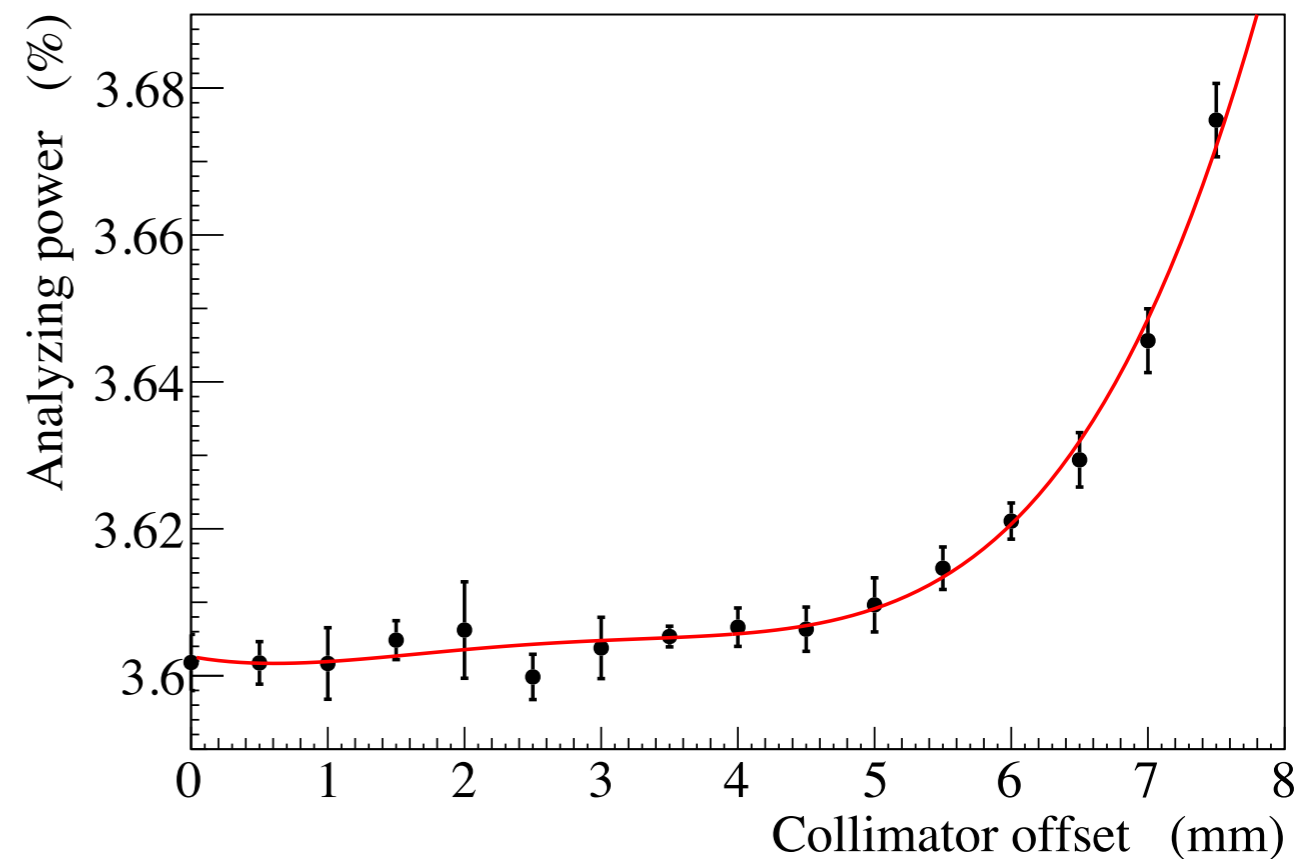
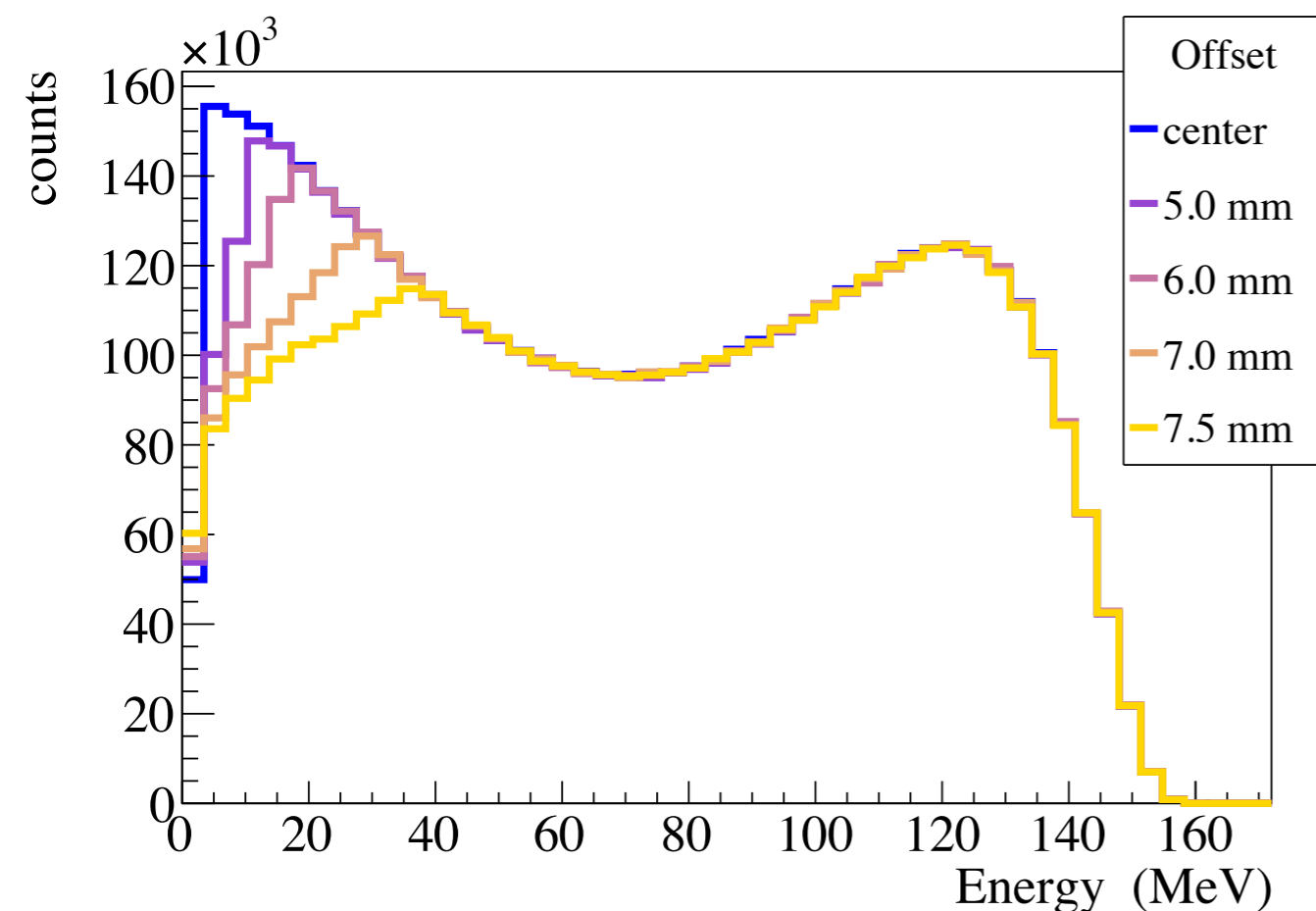


# Photon Detector Response

Simultaneous counting mode DAQ allows detector diagnostics, rate calculations, and for obtaining the energy spectrum of detected photons

Analyzing power determined using MC simulation including realistic photon flux, collimator, detector response and radiative corrections.

Misalignment of the photons on the collimator causes a change in analyzing power.





# Detector linearity and gain stability

Nonlinearity tested in-situ using pulsed LEDs

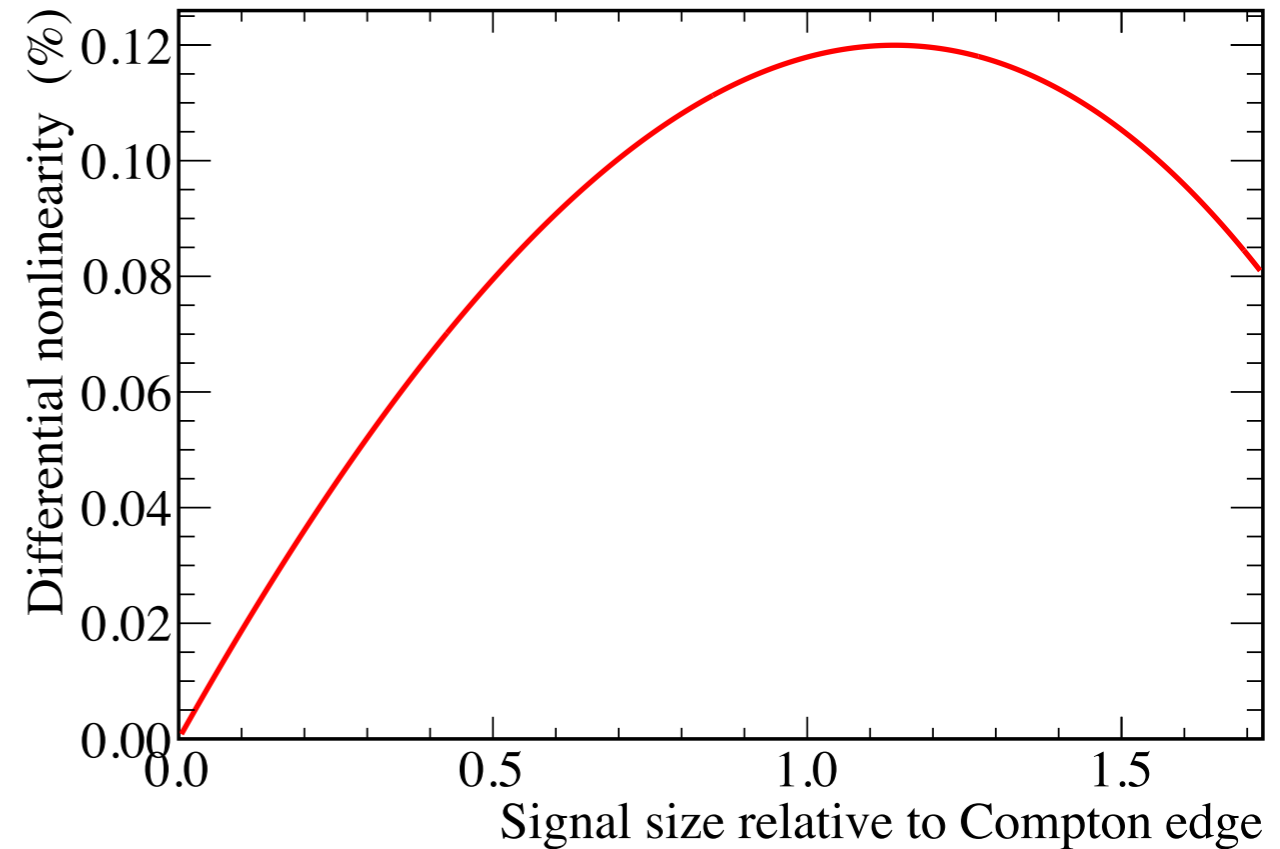
2 LEDs: 1 variable and 1 constant flash together and separately

Finite difference non-linearity

$$\epsilon = \frac{Y(V + \Delta) - Y(V)}{Y(\Delta)}$$

parameters fit to the measured finite-difference non-linearity

Correction applied in MC simulation of  $A_p$



3<sup>rd</sup> LED used to study potential gain shift: change in PMT gain as a function of total brightness

$$\alpha = \frac{Y_{\text{ON}}^{\Delta} - Y_{\text{OFF}}^{\Delta}}{Y_{\text{OFF}}^{\Delta}} \text{ with } \alpha < 0.012$$

$$\langle A_{\text{corr}} \rangle = \frac{\langle A_{\text{exp}} \rangle + \alpha f \Delta_{\text{OFF}}}{1 + \alpha f Y_{\text{OFF}}} \text{ with } f = \frac{1}{Y_{\text{ON}} - Y_{\text{OFF}}}.$$

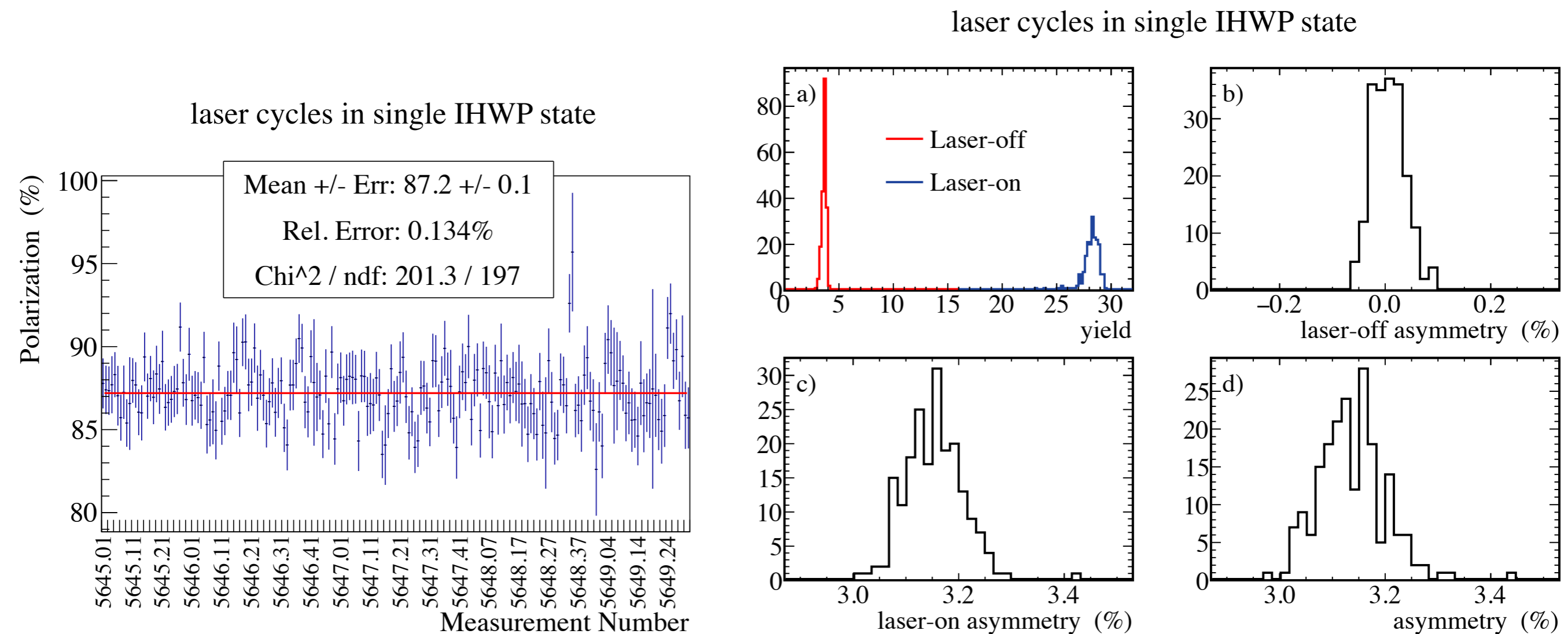
# Systematic Uncertainties

Source	dP/P(%)
Laser polarization	0.25
Collimated spectrum distortion	0.20
Detector gain shift	0.15
Beam energy	0.05
Helicity state polarization difference	0.03
Detector nonlinearity	0.02
Averaging timescale	0.02
Position differences	0.01
<b>Total</b>	<b>0.36</b>

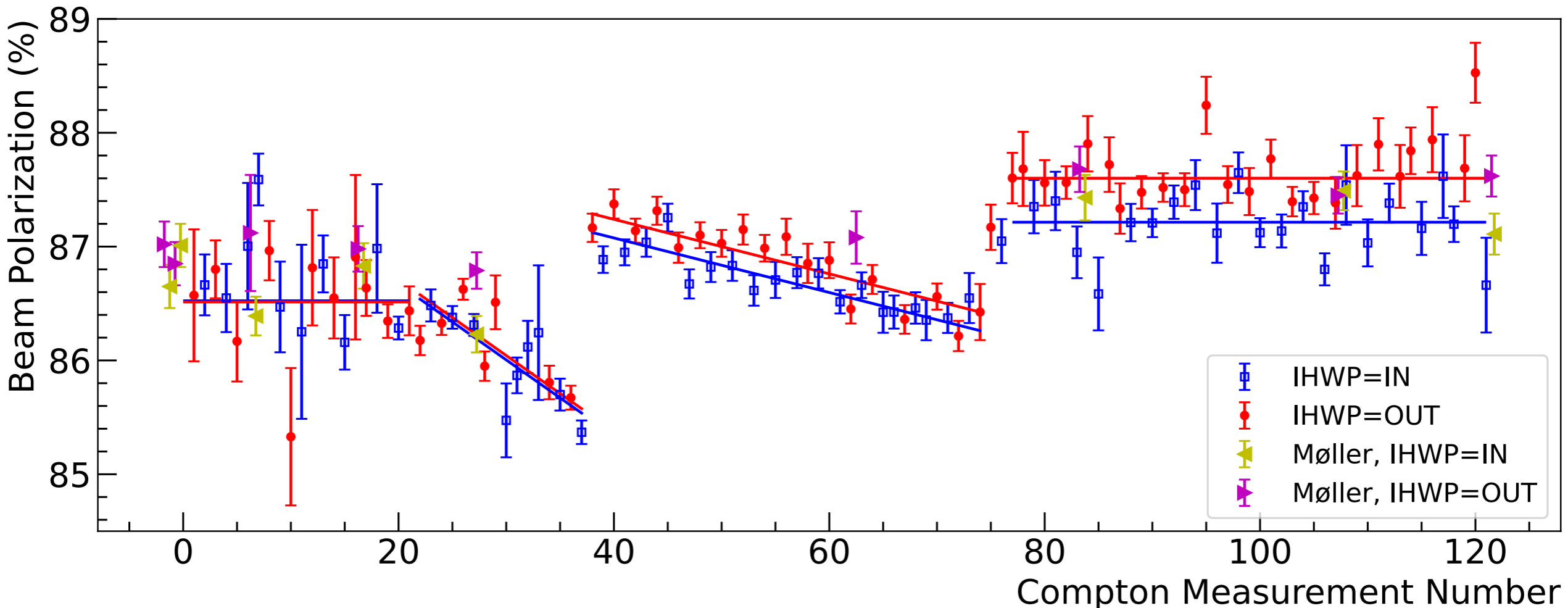
# Data Analysis

14,498 laser cycles passed data quality cuts on pedestal stability, minimum signal size, minimum statistical power, consistent laser-off asymmetry, and small charge-asymmetry

Laser cycles are combined in periods of constant helicity sign (IHWP).



# CREX Polarization



$$86.90 \pm 0.31 \% \text{ (syst)} \pm 0.02 \% \text{ (stat)}$$

Average over the polarization measurements weighted by the main CREX measurement taken in the same time period

Consistent with Moller polarization measurements ( $dP/P = 0.85 \%$ )

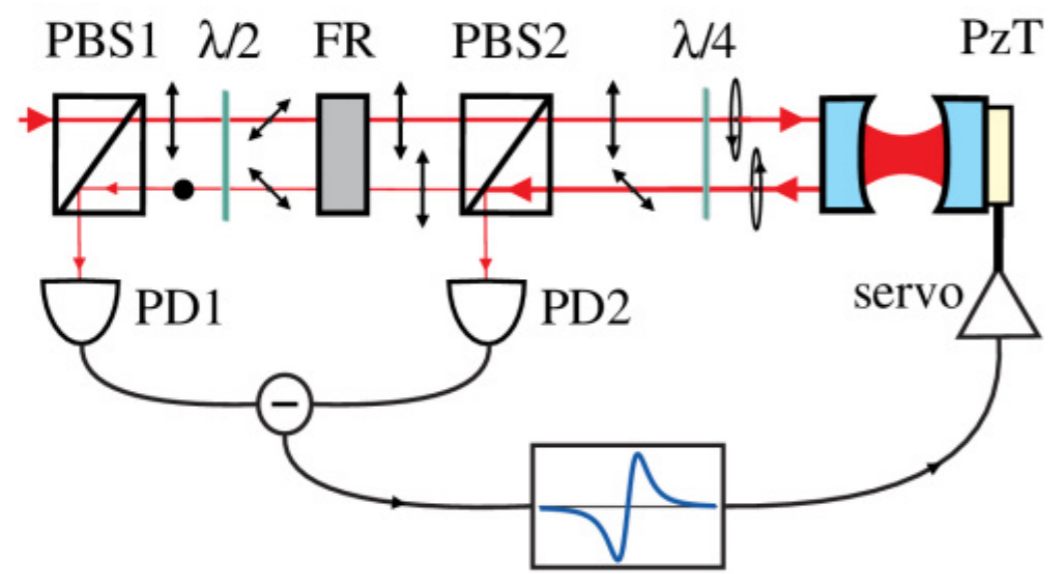
D. E. King et al., [Nucl. Instrum. Methods Phys. Res. A 1045, 167506 \(2023\)](#)

# Future Directions

Higher energy gives larger asymmetries and energy transfer.  
Should provide similar or improved control of systematic uncertainties.  
Electron and photon detector in tandem.  
Fast switching of helicity (2 KHz).

## Laser

Minimize slow drifts  
Implement power-balanced detection scheme



P. Asenbaum and M. Arndt, *Opt. Lett.* **36**, 3720 (2011)

## Electron Detector

New detector required  
Currently in development  
6 cm long active area to capture spectrum  
2 potential detectors technologies: diamond strip or HVMAPS (silicon pixel) detectors  
Improved DAQ

## Photon Detector

Much higher energy  $\sim 3$  GeV  
New detector: lead tungstate crystals  
Update DAQ to newer hardware with same integrating functionality and greatly improved counting functionality

# Summary

Electron beam polarization during CREX was continuously measured to accuracy  $dP/P = 0.36\%$

Most accurate electron beam polarimetry measurement thus far.

Controlled systematic uncertainties from photon detector and laser.

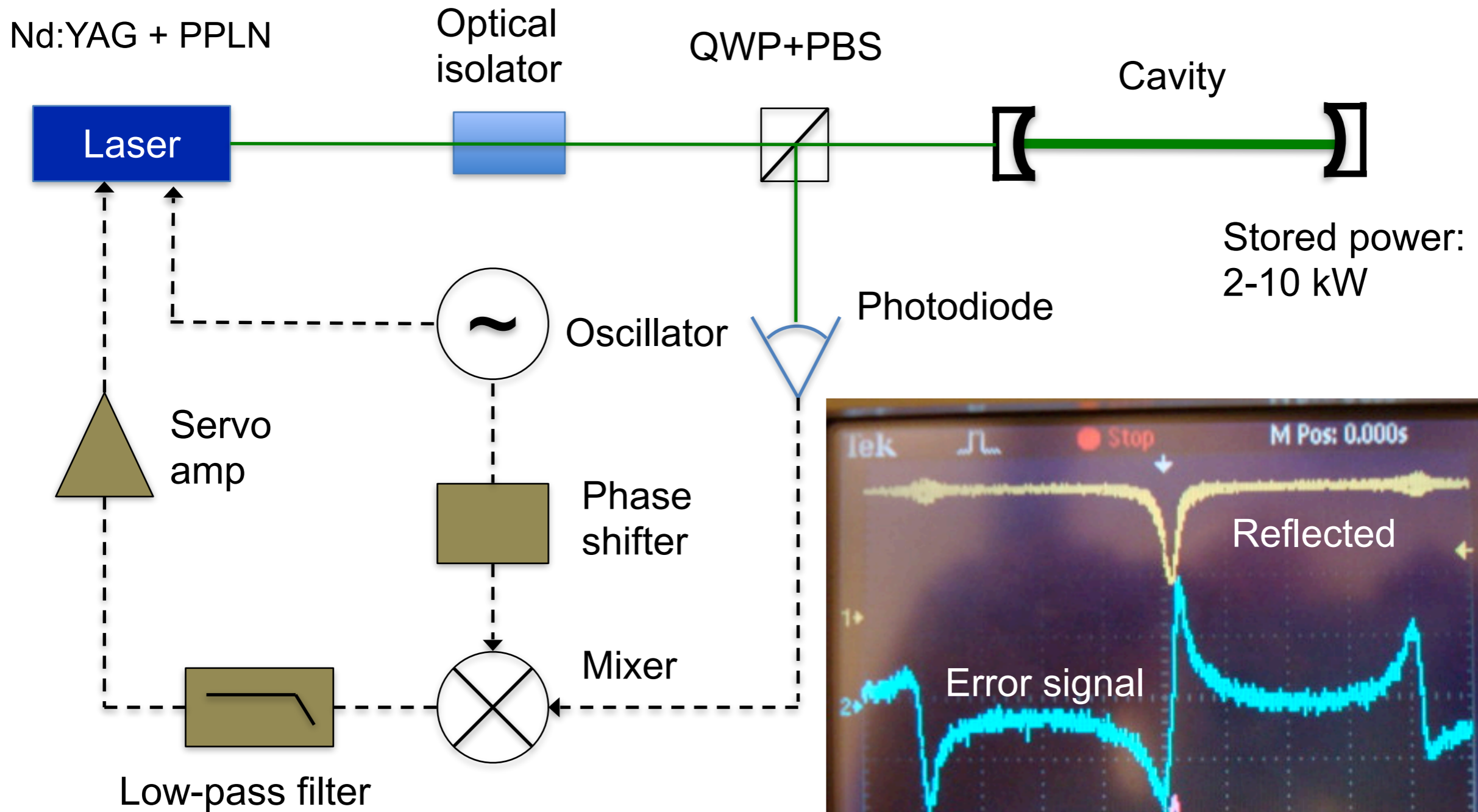
New effects observed related to cavity birefringence and laser table slow drifts.

There is a clear path forward to achieve the precision for MOLLER and SOLID experiments.

# Fabry-Pérot Cavity

- Compton polarimeter measurement time a challenge at JLab
  - Example: At 1 GeV and 180  $\mu\text{A}$ , a 1% (statistics) measurement with 10 W CW laser would take on the order of 1 day!
  - Not much to be gained with pulsed lasers given JLab beam structure (nearly CW)
- A high-finesse (high-gain) Fabry-Pérot cavity locked to narrow linewidth laser is capable of storing several kW of CW laser power
  - First proposed for use at JLab in mid-90's, implemented in Hall A in late 90's (Hall C in 2010, HERA..)
- Fabry-Pérot cavity poses significant challenge in determining laser polarization
  - Degree of circular polarization in cavity can be different than input laser DOCP
  - Vacuum system can introduce additional birefringence

# Fabry-Pérot Cavity



CW laser (1 or 10 W) @ 532 nm locked to low gain, external Fabry-Pérot cavity via Pound-Drever-Hall technique





# Laser Polarization – the “Entrance” Function

Propagation of light into the Fabry-Pérot cavity can be described by matrix,  $M_E$

- Light propagating in opposite direction described by transpose matrix,  $(M_E)^T$
- If input polarization ( $\epsilon_1$ ) linear, polarization at cavity ( $\epsilon_2$ ) circular only if polarization of reflected light ( $\epsilon_4$ ) linear and orthogonal to input\*

